Magnetic properties and ^{61}Ni Mössbauer spectroscopy of the ternary phosphide CrNiP

2008 J. Phys.: Condens. Matter 20 285227

(http://iopscience.iop.org/0953-8984/20/28/285227)

J. Phys.: Condens. Matter **20** (2008) 285227 (7pp) doi:10.1088/0953-8984/20/28/285227

Magnetic properties and ^{61}Ni Mössbauer spectroscopy of the ternary phosphide CrNiP

Z M Stadnik[1,4], P Wang[1], N Jansen[2], D Walcher[2], P Gütlich[2] and T Kanomata[3]

[1] Department of Physics, University of Ottawa, Ottawa, ON, K1N 6N5, Canada
[2] Institut für Anorganische Chemie und Analytische Chemie, Johannes Gutenberg Universität, 55099 Mainz, Germany
[3] Faculty of Engineering, Tohoku Gakuin University, Tagajo, Miyagi 985-8537, Japan

E-mail: stadnik@uottawa.ca

Received 11 April 2008, in final form 30 May 2008
Published 24 June 2008
Online at stacks.iop.org/JPhysCM/20/285227

Abstract

The results of x-ray diffraction, dc magnetization, and ^{61}Ni Mössbauer spectroscopy studies of the ternary phosphide CrNiP are reported. This compound crystallizes in the orthorhombic Co_2P-type structure (space group *Pnma*) with the lattice parameters $a = 5.7965(1)$ Å, $b = 3.5337(1)$ Å, and $c = 6.8123(2)$ Å. NiCrP is a ferromagnet with Curie temperature $T_C = 135.1(1)$ K. The ferromagnetic-to-paramagnetic transition is characterized by the critical exponents $\beta = 0.355(22)$, $\gamma = 1.241(18)$, and $\delta = 4.585(20)$. Their values are close to those of a 3D Heisenberg ferromagnet. The temperature dependence of the magnetic susceptibility above T_C follows the modified Curie–Weiss law with a paramagnetic Curie temperature of 142.9(6) K and effective magnetic moment per transition-metal atom of 1.70(2) μ_B. The magnetic moment per formula unit at 4.2 K is found to be 0.816(13) μ_B. The hyperfine magnetic field at ^{61}Ni nuclei at 4.2 K of 32.3(1.3) kOe implies that the Ni atoms carry a magnetic moment of 0.14(8) μ_B, and that the moment carried by the Cr atoms is 0.68(9) μ_B. The Debye temperature of NiCrP is 261(3) K.

(Some figures in this article are in colour only in the electronic version)

1. Introduction

The crystallographic and magnetic properties of the ternary transition-metal phosphides $(T_{1-x}T'_x)_2P$ (T, T′ = transition metal) have been the subject of numerous investigations [1]. These ternary compounds crystallize in two different crystal structure types: the orthorhombic Co_2P-type structure and the hexagonal Fe_2P-type structure. These two structure types have a common sub-cell where there are two kinds of transition-metal sites: the tetrahedral site surrounded by four P atoms and the pyramidal site surrounded by five P atoms. The phosphides $(T_{1-x}T'_x)_2P$ show almost all possible types of magnetic ordering: ferromagnetism, antiferromagnetism, canted antiferromagnetism, and paramagnetism. The ternary phosphides containing Ni, $(Fe_{1-x}Ni_x)_2P$ [2–9] and $(Cr_{1-x}Ni_x)_2P$ [10, 11], are ferromagnets. It has been argued both qualitatively [3] and theoretically [4, 7, 12, 13] that Ni atoms in these phosphides carry a negligible magnetic moment, i.e., that the magnetic moment is carried solely by Fe or Cr atoms.

The ternary phosphide CrNiP is an itinerant ferromagnet with the Curie temperature, T_C, of 140–146 K and the magnetic moment per formula unit, μ_{FU}, of 0.83–0.85 μ_B [10, 11, 14]. It has been argued theoretically on the basis of a narrow *d*-band model [12] that Ni atoms in CrNiP carry no magnetic moment and that all the moment is carried by Cr atoms. On the other hand, electronic band structure calculations predict [13] that in the phosphide CrNiP, Ni atoms carry a non-zero magnetic moment of 0.06 μ_B and Cr atoms carry a magnetic moment of 0.97 μ_B.

[4] Author to whom any correspondence should be addressed.

The above controversy concerning the Ni magnetic moment in CrNiP can be resolved by using experimental techniques which probe this moment directly, such as the rarely used ^{61}Ni nuclear magnetic resonance (NMR) or ^{61}Ni Mössbauer effect (ME). If there exists a magnetic moment on the Ni atoms in CrNiP, the hyperfine magnetic field at ^{61}Ni nuclei determined from ^{61}Ni NMR or ^{61}Ni ME spectra must have a non-zero value. In this paper, we report on structural, magnetic, and ^{61}Ni ME studies of the ternary phosphide CrNiP.

2. Experimental procedure

A polycrystalline sample of CrNiP was prepared from powders of Cr, Ni, and P with purities of 99.99%, 99.99%, and 99.999%, respectively. The powders were mixed in the desired proportion, sealed in an evacuated silica tube and annealed at 873 K for 2 days and then quenched. The reaction product was next subjected to a vacuum heat treatment at 1073 K for 2 days and then quenched. Finally, the ingot was pulverized, mixed well and heated again in vacuum at 1173 K for 7 days and then quenched.

X-ray diffraction measurements were performed at 298 K in the Bragg–Brentano geometry on the PANanalytical X'Pert scanning diffractometer using Cu Kα radiation. The Kβ line was eliminated by using a Kevex PSi2 Peltier-cooled solid-state Si detector. In order to avoid the deviation from intensity linearity of the solid-state Si detector, its parameters and the parameters of the diffractometer were chosen in such a way as to limit the count rate from the most intense Bragg peaks to less than 9000 counts s^{-1} [15].

The magnetic measurements were carried out with a Quantum Design superconducting quantum interference device magnetometer at various fields in the temperature range 5.0–300 K.

The ^{61}Ni ME measurements were conducted using a standard Mössbauer spectrometer operating in sine mode, using the 67.4 keV transition in ^{61}Ni [16, 17]. Both the source and the absorber were in direct contact with liquid helium in a cryostat. The spectrometer was calibrated with a 6.35 μm-thick α-Fe foil [18], and the spectra were folded. The single line sources of ^{61}Co (half life = 99 min) in $^{62}Ni_{0.85}Cr_{0.15}$ (^{62}Ni enriched to 97.7%) were activated in the MAinz MIcrotron (MAMI) using the nuclear reaction ^{62}Ni(γ, p)^{61}Co, with bremsstrahlung including the giant resonance region of 20–25 MeV necessary for this nuclear reaction to occur. A pneumatic tube approximately 50 m long was used to transport small platelets (4 × 4 mm^2) of $^{62}Ni_{0.85}Cr_{0.15}$ to the activation position. Immediately after an activation of about 2 h, the radioactive source material was pneumatically ejected and transported into a cryostat in which the Mössbauer absorber was already cooled to 4.2 K. Three sources had to be used to obtain a Mössbauer spectrum of sufficient signal-to-noise ratio. The Mössbauer absorber was made of pulverized material pressed into a Teflon sample holder. The surface density of the Mössbauer absorber of the CrNiP alloy was 719 mg cm^{-2}. The 67.4 keV γ-rays were detected with a 2.0 mm NaI(Tl) scintillation detector.

The measured ^{61}Ni Mössbauer spectrum was analyzed by means of a least-squares fitting procedure which entailed calculations of the positions and relative intensities of the absorption lines by numerical diagonalization of the full hyperfine interaction Hamiltonian. In the principal axis system of the electric field gradient (EFG) tensor, the Hamiltonian can be written as [16, 17]

$$\hat{H} = g\mu_N H_{hf}\left[\hat{I}_z\cos\theta + \frac{1}{2}\left(\hat{I}_+ e^{-i\phi} + \hat{I}_- e^{i\phi}\right)\sin\theta\right] + \frac{eQV_{zz}}{4I(2I-1)}\left[3\hat{I}_z^2 - I(I+1) + \frac{\eta}{2}\left(\hat{I}_+^2 + \hat{I}_-^2\right)\right], \quad (1)$$

where g is a nuclear g-factor of a nuclear state, μ_N is the nuclear Bohr magneton, H_{hf} is the hyperfine magnetic field at a nuclear site, e is the proton charge, Q is the quadrupole moment of a nuclear state, I is the nuclear spin, V_{zz} is the z component of the EFG tensor, η is the asymmetry parameter defined as $\eta = |(V_{xx} - V_{yy})/V_{zz}|$ (if the principal axes are chosen such that $|V_{xx}| < |V_{yy}| < |V_{zz}|$, then $0 \leqslant \eta \leqslant 1$), θ is the angle between the direction of H_{hf} and the V_{zz}-axis, ϕ is the angle between the V_{xx}-axis and the projection of H_{hf} onto the xy plane, and the $\hat{I}_z$, $\hat{I}_+$, and $\hat{I}_-$ operators have their usual meaning. During the fitting procedure, the g factors and the quadrupole moments for ^{61}Ni ($I_g = 3/2$, $I_{ex} = 5/2$) were constrained to $g_{ex} = 0.1905$ and $g_g = -0.499\,87$, and $Q_{ex} = -0.196b$ and $Q_g = 0.162b$, respectively [19].

The resonance line shape of the Mössbauer spectra was described by a transmission integral formula [20, 21]. In addition to the hyperfine parameters, only the absorber Debye–Waller factor f_a and the absorber linewidth Γ_a were fitted as independent parameters. The source linewidth $\Gamma_s = 0.440$ mm s^{-1} and the background-corrected Debye–Waller factor of the source $f_s^* = 0.11$ [22], were used in the fit.

3. Results and discussion

3.1. Structural characterization

The ternary phosphide CrNiP forms in the Co_2P-type crystal structure with the space group $Pnma$ (No. 62). Three different 4c positions (x, $\frac{1}{4}$, z) are occupied by Cr, Ni, and P, respectively, which correspond to four formula units of CrNiP per unit cell. The crystal structure of CrNiP is shown in figure 1. The Cr atoms are pyramidally coordinated by five P atoms and the Ni atoms are tetrahedrally coordinated by four P atoms.

The x-ray powder diffraction pattern of the sample studied is shown in figure 2. A Rietveld refinement of the x-ray powder diffraction data was performed yielding the lattice parameters $a = 5.7965(1)$ Å, $b = 3.5337(1)$ Å, and $c = 6.8123(2)$ Å. The obtained atomic positions for the Cr, Ni, and P sites are listed in table 1 and the interatomic distances are listed in table 2. The sample studied contains traces of second phases of CrNiP (space group $P\bar{6}2m$ [23]) in the amount of 9.7(3) wt% and of Cr_2O_3 (space group $R\bar{3}c$) in the amount of 1.8(2) wt%, as determined from the Rietveld refinement of the x-ray powder diffraction pattern (figure 2).

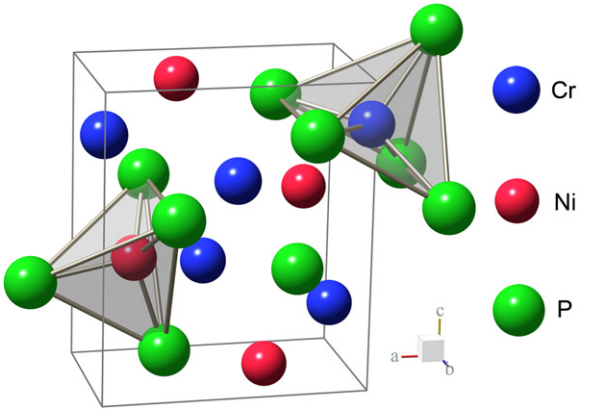

Figure 1. Crystal structure of CrNiP. The pyramidal and tetrahedral coordinations of the Cr and Ni atoms are indicated.

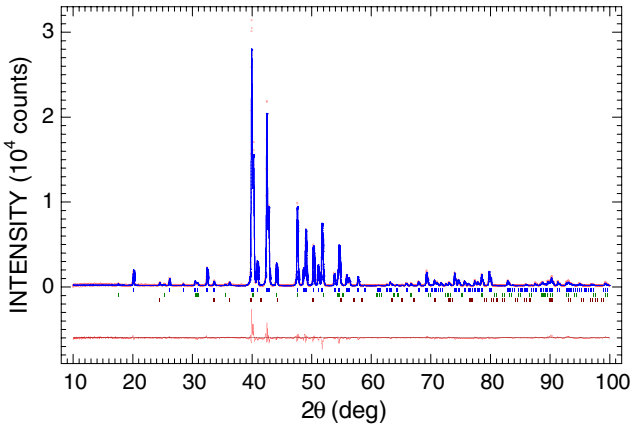

Figure 2. The x-ray powder diffraction spectrum of CrNiP at 298 K. The experimental data are denoted by open circles, while the line through the circles represents the results of the Rietveld refinement. The upper set of vertical bars represents the Bragg peak positions corresponding to the principal CrNiP phase, while the lower two sets refer to the positions of the minor impurity phases of CrNiP (space group $P\bar{6}2m$ [23]) and Cr_2O_3 (space group $R\bar{3}c$). The lower curve shows the difference between the experimental data and the calculated curve.

Table 1. Atomic positions for the orthorhombic phosphate CrNiP obtained through Rietveld analysis.

Atom	Site	Point symmetry	x	y	z	Occupancy
Cr	4c	m	0.0271(3)	$\frac{1}{4}$	0.1673(2)	1.0
Ni	4c	m	0.1423(2)	$\frac{1}{4}$	0.5642(2)	1.0
P	4c	m	0.7608(5)	$\frac{1}{4}$	0.6274(3)	1.0

3.2. Magnetic properties

The temperature dependence of the magnetization M of CrNiP measured in an applied magnetic field of 15 kOe between 5.0 and 300 K is shown in figure 3. This phosphide is obviously a ferromagnet. For a mean-field ferromagnet, $M^2 \propto T_C - T$ near T_C [24]. From a linear fit of M^2 versus T (inset in figure 3), T_C was estimated to be 152.7(1.2) K.

The temperature dependence of the inverse magnetic susceptibility χ of CrNiP is shown in figure 4. In the

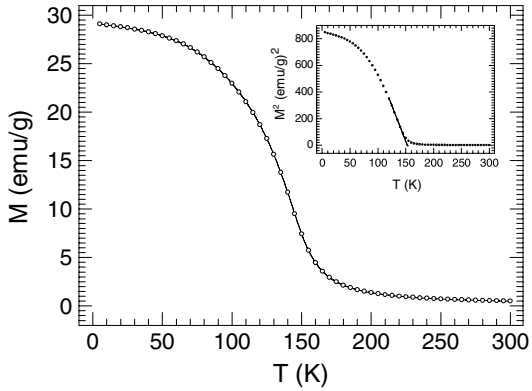

Figure 3. The temperature dependence of the magnetization of CrNiP, measured in an external magnetic field of 15 kOe. The solid line is a guide for the eye. The inset shows the temperature dependence of the square of the magnetization and the solid line is a linear fit of the data around T_C.

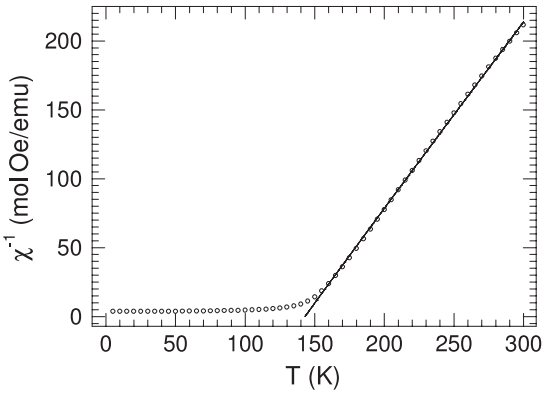

Figure 4. The temperature dependence of the inverse magnetic susceptibility of CrNiP, measured in an external magnetic field of 15 kOe. The solid line is the fit to equation (2) in the temperature range 150–300 K.

Table 2. Interatomic distances (in Å) for the orthorhombic phosphate CrNiP.

Cr		Ni		P	
1P	2.424(3)	1P	2.210(3)	1Ni	2.210(3)
2P	2.446(2)	1P	2.253(3)	1Ni	2.253(3)
2P	2.566(2)	2P	2.267(2)	2Ni	2.267(2)
2Ni	2.700(2)	2Ni	2.571(1)	1Cr	2.424(3)
2Ni	2.726(1)	2Cr	2.700(2)	2Cr	2.446(2)
1Ni	2.730(2)	2Cr	2.726(1)	2Cr	2.566(2)
1Ni	2.785(2)	1Cr	2.730(2)	2P	3.344(4)
2Cr	2.901(1)	1Cr	2.785(2)	1Cr	3.493(3)
2Cr	3.109(2)				
1P	3.493(3)				

paramagnetic region the $\chi(T)$ data could be fitted to a modified Curie–Weiss law

$$\chi = \chi_0 + \frac{C}{T - \theta_p}, \tag{2}$$

where χ_0 is the temperature independent magnetic susceptibility, C is the Curie constant, and θ_p is the paramagnetic

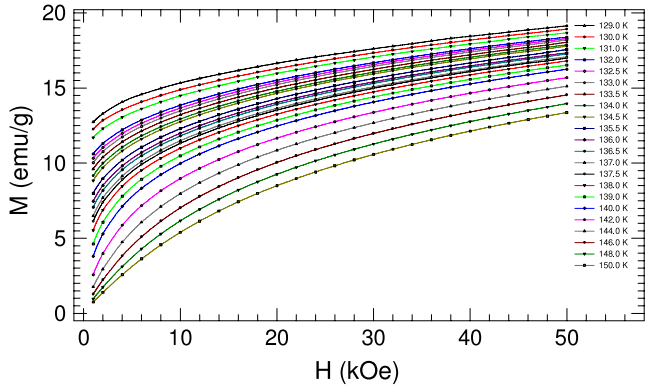

Figure 5. The magnetization isotherms versus the magnetic field at temperatures between 129 and 150 K. The solid lines are guides for the eye.

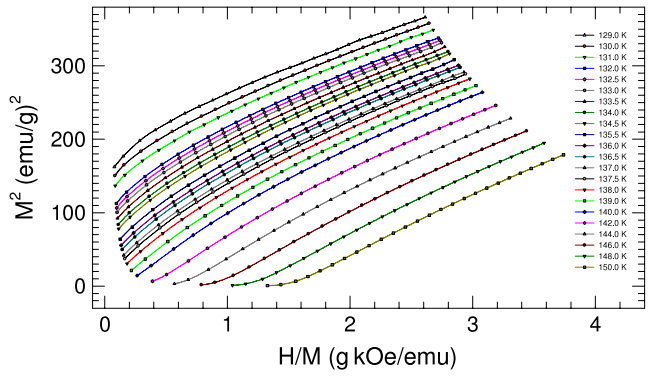

Figure 6. The Arrott plot for CrNiP. The solid lines are guides for the eye.

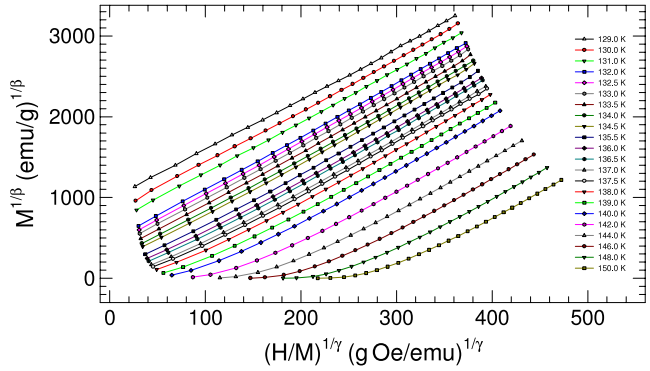

Figure 7. The modified Arrott plot for CrNiP with $\beta = 0.365$ and $\gamma = 1.336$. The solid lines are guides for the eye.

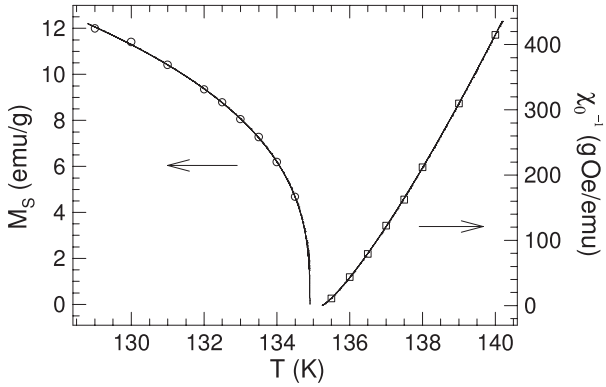

Figure 8. The temperature dependence of the spontaneous magnetization and the inverse initial susceptibility. The solid lines are fits of the experimental data to equations (3) and (4).

Curie temperature. The Curie constant can be expressed as $C = \frac{N\mu_{\rm eff}^2}{3k}$, where N is the concentration of magnetic atoms per unit mass, k is the Boltzmann constant, and $\mu_{\rm eff}$ is the effective magnetic moment. The values of χ_0, C, and θ_p obtained from the fit are 7.67(97) $\times$ 10^{-5} emu Oe^{-1} mol^{-1}, 0.723(13) emu Oe^{-1} K mol^{-1}, and 142.9(6) K, respectively. This value of C corresponds to $\mu_{\rm eff}$ of 1.70(2) $\mu_{\rm B}$ per transition-metal atom. The positive paramagnetic Curie temperature is consistent with the ferromagnetic ordering, and the value of θ_p is close to $T_{\rm C}$.

Figure 5 shows a series of magnetization isotherms measured in the vicinity of $T_{\rm C}$, estimated above. The usual procedure for extracting the spontaneous magnetization $M_{\rm S}(T) = \lim_{H\to 0} M$, the inverse initial susceptibility $\chi_0^{-1} = \lim_{H\to 0}(H/M)$, and $T_{\rm C}$ from the $M(H)$ isotherms is to make use of the Arrott plot [25], M^2 versus H/M. According to mean-field theory, near $T_{\rm C}$ this plot should consist of a series of parallel lines for different temperatures, with the line at $T = T_{\rm C}$ passing through the origin, and the $M_{\rm S}(T)$ and $\chi_0^{-1}(T)$ are determined from the intercept values on the ordinate ($T \leqslant T_{\rm C}$) and abscissa ($T \geqslant T_{\rm C}$), respectively. However, in the present case the curves in the Arrott plot (figure 6) are nonlinear and concave. This shows that CrNiP is not a mean-field ferromagnet. Therefore, we analyzed the $M(H)$ data using a modified Arrott plot [26], in which $M^{1/\beta}$ is plotted versus $(M/H)^{1/\gamma}$, where β and γ are critical exponents defined through the relations [27]

$$M_{\rm S}(T) = M_0(-\varepsilon)^{\beta}, \qquad \varepsilon < 0 \tag{3}$$

$$\chi_0^{-1}(T) = (h_0/M_0)\varepsilon^{\gamma}, \qquad \varepsilon > 0, \tag{4}$$

where $\varepsilon = (T - T_{\rm C})/T_{\rm C}$, and M_0 and h_0/M_0 are the critical amplitudes. At $T_{\rm C}$, a critical exponent δ relates M and H by [27]

$$M = DH^{1/\delta}, \qquad \varepsilon = 0, \tag{5}$$

where D is a critical amplitude. Different values of β and γ were taken as trial values and it was found that the values of $\beta = 0.365$ and $\gamma = 1.336$, which are similar to those of the three-dimensional (3D) magnet [28], resulted in nearly straight lines for sufficiently high fields (figure 7). Using the modified Arrott plot (figure 7), a linear extrapolation of the straight lines of the isotherms from fields above 2.0 kOe to $(M/H)^{1/\gamma} = 0$ and $M^{1/\beta} = 0$ yields intercepts on the $M^{1/\beta}$ and $(M/H)^{1/\gamma}$ axes, respectively, from which the values of $M_{\rm S}(T)$ and $\chi_0^{-1}(T)$ are computed. These values as a function of temperature are plotted in figure 8. The fits of the $M_{\rm S}(T)$ and $\chi_0^{-1}(T)$ data (figure 8) to equations (3) and (4) respectively give $\beta = 0.355(22)$, $T_{\rm C} = 134.91(3)$ K and $\gamma = 1.241(18)$, $T_{\rm C} = 135.24(3)$ K. The value of $T_{\rm C}$ for CrNiP is then taken

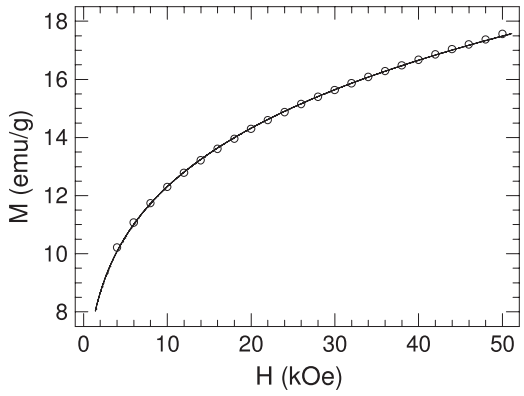

Figure 9. The magnetization isotherm versus the magnetic field at 135.5 K. The solid line is the fit to equation (5).

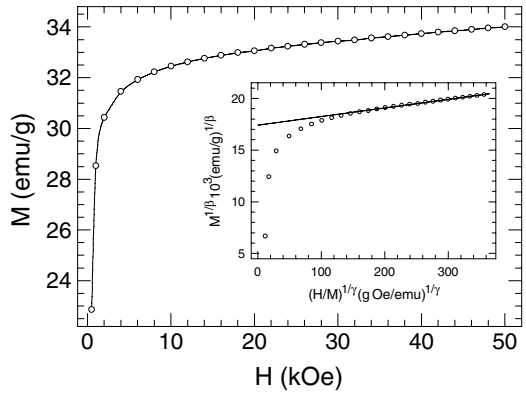

Figure 10. The magnetization isotherm versus the magnetic field at 4.2 K. The solid line is a guide for the eye. The inset shows the modified Arrott plot with $\beta = 0.355$ and $\gamma = 1.241$. The solid line is a linear fit to the high-field data.

as 135.1(1) K. The critical exponents obtained in this way are close to those of the short-range 3D Heisenberg model predictions ($\beta = 0.3689(3)$, $\gamma = 1.3960(9)$) [28].

To obtain the value of δ, we plot M versus H for the closest measured isotherm, 135.5 K, to $T_C = 135.1(1)$ K in figure 9. The fit of this isotherm to equation (5) (figure 9) gives $\delta = 4.585(20)$. This value is close to the value of $\delta = 4.783(3)$ expected [28] for a 3D Heisenberg ferromagnet.

The critical exponents β, γ, and δ should fulfill the Widom exponent relation [29] $\gamma - \beta(\delta - 1) = 0$. The determined values of β, γ, and δ satisfy this relation well ($-0.103(108)$), within experimental error.

The magnetic field dependence of the magnetization measured at 4.2 K is shown in figure 10. The magnetization does not saturate, even in a field of 50 kOe. The saturation magnetization at 4.2 K was obtained from a modified Arrott plot (inset in figure 10) by a linear extrapolation of the high-field data to $(M/H)^{1/\gamma} = 0$. This yielded $M_S = 32.17(53)$ emu g^{-1}, which corresponds to the magnetic moment per formula unit $\mu_{FU} = 0.816(13)\ \mu_B$, or to the magnetic moment per transition metal (TM) (assuming that P atoms carry no magnetic moment) $\mu_{TM} = 0.408(7)\ \mu_B$.

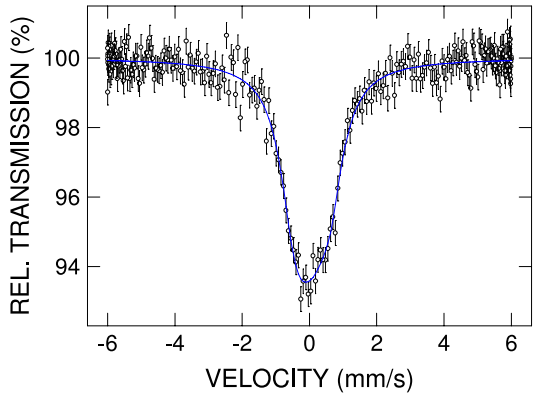

Figure 11. The ^{61}Ni Mössbauer spectrum of CrNiP measured at 4.2 K. The solid line is a fit, as described in the text. The zero-velocity origin is relative to the source.

3.3. Mössbauer spectroscopy

Figure 11 shows a ^{61}Ni Mössbauer spectrum of CrNiP measured at 4.2 K. The Ni atoms are located in the crystal structure at the site with the point symmetry m (table 1). This ensures a non-zero electric field gradient at the Ni site and hence a possible non-zero electric quadrupole splitting. The spectrum in figure 11 clearly exhibits the presence of a poorly resolved hyperfine magnetic interaction. It was fitted with the transmission integral by diagonalization of the hyperfine Hamiltonian (equation (1)). The following values of the hyperfine parameters were inferred from the fit: $\Gamma_a = 0.399(8)$ mm s^{-1}, the isomer shift (relative to the ^{61}Co(Ni$_{0.85}$Cr$_{0.15}$) source) $\delta = 0.017(15)$ mm s^{-1}, $V_{zz} = -0.137(81) \times 10^{22}$ V m^{-2}, $f_a = 6.9(2)\%$ and $H_{hf} = 32.3(1.3)$ kOe.

The value of Γ_a is only slightly larger than the natural linewidth $\Gamma_{nat} = 0.385$ mm s^{-1} [19], as expected. Similarly to what has been found for other metallic systems [17, 30], the values of δ and V_{zz} are essentially equal to zero. In terms of the Debye approximation for the lattice vibrations, the absorber Debye–Waller factor f_a is expressed [16, 17] by the Debye temperature, Θ_D, as

$$f_a(T) = \exp\left\{-\frac{3}{4}\frac{E_\gamma^2}{Mc^2k\Theta_D} \times \left[1 + \left(\frac{T}{\Theta_D}\right)^2 \int_0^{\Theta_D/T} \frac{x\,dx}{e^x - 1}\right]\right\}, \quad (6)$$

where E_γ is the energy of the Mössbauer transition, M is the mass of the Mössbauer nucleus, c is the speed of light, and k is the Boltzmann constant. The value of f_a obtained from the fit via equation (6) yields $\Theta_D = 261(3)$ K.

A non-zero value of H_{hf} implies a non-zero value of the nickel magnetic moment μ_{Ni} in CrNiP. There is no firmly established relationship between the measured H_{hf} and μ_{Ni}. There are two major contributions to H_{hf} at the nuclei of TM elements in metallic alloys [16, 17]: the core contribution, due to the polarization of core s electrons and the polarization of the conduction electrons by the 3d electrons (i.e., by the on-site magnetic moment), and the conduction

electron contribution, due to the polarization of the conduction electrons by the surrounding magnetic moments. The first contribution is proportional to the local magnetic moment μ_l, whereas the second contribution is assumed to be proportional to the average moment per magnetic atom μ_{TM} Thus, a phenomenological relation is used [31]

$$H_{hf} = a\mu_l + b\mu_{TM}, \tag{7}$$

where a and b are assumed to be constant for a given alloy system. This relation enables one to estimate the value of μ_l from the measured values of H_{hf} and μ_{TM}, provided that the values of a and b are known from an earlier calibration. Due to the scarcity of data on the values of H_{hf} at ^{61}Ni nuclei in Ni-containing alloys, the values of a and b are known only for a few alloy series [32–36]. From an earlier calibration for the ternary pnictide CrNiAs for which the Ni magnetic moment is known from the neutron diffraction study, we found that $a = 63(5)$ kOe/μ_B and $b = 57(5)$ kOe/μ_B [37]. Using the value of μ_{TM} determined above and the measured value of H_{hf}, one obtains $\mu_{Ni} = 0.14(8)$ μ_B from equation (7). It is thus concluded that the Ni atoms in the CrNiP ferromagnet do carry a magnetic moment. This finding is at variance with the theoretical prediction of $\mu_{Ni} = 0$ in CrNiP [12] and in agreement with the prediction based on the electronic structure calculations of the non-zero μ_{Ni} in CrNiP [13]. Since the Ni and Cr magnetic moments are coupled ferromagnetically in CrNiP, the values of $\mu_{Ni} = 0.14(8)$ μ_B and $\mu_{FU} = 0.816(13)$ μ_B imply that the Cr atoms carry a magnetic moment of 0.68(9) μ_B.

4. Conclusions

The ternary phosphide CrNiP has been studied by means of x-ray diffraction, magnetization measurements, and ^{61}Ni Mössbauer spectroscopy. The studied compound has the orthorhombic Co_2P-type structure (space group *Pnma*) with the lattice parameters $a = 5.7965(1)$ Å, $b = 3.5337(1)$ Å, and $c = 6.8123(2)$ Å. The Curie temperature T_C is found to be 135.1(1) K and three critical exponents are determined $\beta = 0.355(22)$, $\gamma = 1.241(18)$, and $\delta = 4.585(20)$. The values of these critical exponents are close to those of a 3D Heisenberg ferromagnet. The temperature dependence of the magnetic susceptibility above T_C follows the modified Curie–Weiss law with the paramagnetic Curie temperature of 142.9(6) K and the effective magnetic moment per transition-metal atom of 1.70(2) μ_B. The magnetic moment per formula unit at 4.2 K is found to be 0.816(13) μ_B. The hyperfine magnetic field of 32.3(1.3) kOe at ^{61}Ni nuclei at 4.2 K implies that the Ni atoms carry a magnetic moment of 0.14(8) μ_B, and that the moment carried by the Cr atoms is 0.68(9) μ_B. The Debye temperature of CrNiP is 261(3) K.

Acknowledgment

This work was supported by the Natural Sciences and Engineering Research Council of Canada.

References

[1] Beckman O and Lundgren L 1991 *Handbook of Magnetic Materials* vol 6, ed K H J Buschow (Amsterdam: Elsevier) p 181
[2] Fruchart R, Roger A and Senateur J P 1969 *J. Appl. Phys.* **40** 1250
[3] Fuji H, Hōkabe T, Fujiwara H and Okamoto T 1978 *J. Phys. Soc. Japan* **44** 96
[4] Kaprzyk S, Nizioł S, Toboła J, Zach R, Bacmann M, Fruchart D and Wolfers P 1997 *Acta Phys. Pol.* A **91** 475
[5] Kumar S, Paranjpe S K, Srivastava B K and Krishnamurthy A 1999 *Phys. Status Solidi* a **175** 693
[6] Średniawa B, Duraj R, Pacyna A, Bombik A, Zach R, Bacmann M, Fruchart D, Nizioł S, Fornal P and Stanek J 2000 *Acta Phys. Pol.* A **97** 921
[7] Zach R, Toboła J, Średniawa B, Kaprzyk S, Casado C, Bacmann M and Fruchart D 2004 *J. Alloys Compounds* **383** 322
[8] Fruchart D, Allab F, Balli M, Gignoux D, Hlil E K, Koumina A, Skryabina N, Tobola J, Wolfers P and Zach R 2005 *Physica* A **358** 123
[9] Balli M, Fruchart D, Gignoux D, Tobola J, Hlil E K, Wolfers P and Zach R 2007 *J. Magn. Magn. Mater.* **316** 358
[10] Iwata N, Matsushima T, Fujii H and Okamoto T 1981 *J. Phys. Soc. Japan* **50** 729
[11] Kanomata T, Endo H, Yamauchi H, Yamaguchi Y, Yoshida H, Kaneko T, Aruga Katori H and Goto T 1997 *Physica* B **237/238** 517
[12] Goodenough J B 1973 *J. Solid State Chem.* **7** 428
[13] Ishida S, Takiguchi T, Fujii S and Asano S 1996 *Physica* B **217** 87
[14] Nylund M A, Roger A, Sénateur J P and Fruchart R 1972 *J. Solid State Chem.* **4** 115
[15] Bish D L and Chipera S J 1989 *Powder Diffr.* **4** 137
[16] Greenwood N N and Gibb T C 1971 *Mössbauer Spectroscopy* (London: Chapman and Hall)
[17] Gütlich P, Link R and Trautwein A 1978 *Mössbauer Spectroscopy and Transition Metal Chemistry* (Berlin: Springer)
[18] Cali J P (ed) *Certificate of Calibration, Iron Foil Mössbauer Standard,* NBS (US) Circular No. 1541 (Washington, DC: US Government Printing Office)
[19] Stevens J G 1981 *CRC Handbook of Spectroscopy* vol 3, ed J W Robinson (Boca Raton, FL: CRC Press) p 403
[20] Margulies S and Ehrman J R 1961 *Nucl. Instrum. Methods* **12** 131
[21] Shenoy G K, Friedt J M, Maletta H and Ruby S L 1974 *Mössbauer Effect Methodology* vol 10, ed I J Gruverman, C W Seidel and D K Dieterly (New York: Plenum) p 277
[22] Rummel H 1982 ^{61}Ni-Mössbauer-Untersuchungen der Magnetischen Hyperfeinfelder in Nickelspinellen *PhD Thesis* Johannes Gutenberg-Universität, Mainz
[23] Orishchin S V and Kuz'ma Yu B 1984 *Inorg. Mater.* **20** 360
[24] Zijlstra H 1967 *Experimental Methods in Magnetism* vol 2 (Amsterdam: North-Holland)
[25] Arrott A 1957 *Phys. Rev.* **108** 1394
[26] Arrott A and Noakes J E 1967 *Phys. Rev. Lett.* **19** 786
[27] Stanley H E 1971 *Introduction to Phase Transitions and Critical Phenomena* (New York: Oxford University Press)
[28] Campostrini M, Hasenbusch M, Pelissetto A, Rossi P and Vicari E 2002 *Phys. Rev.* B **65** 144520
[29] Widom B 1964 *J. Chem. Phys.* **41** 1633
Widom B 1965 *J. Chem. Phys.* **43** 3898
[30] Tomala K, Czjzek G, Fink J and Schmidt H 1977 *Solid State Commun.* **24** 857

[31] Johnson C E, Ridout M S and Cranshaw T E 1963 *Proc. Phys. Soc.* **81** 1079
Collins M F and Wheeler D A 1963 *Proc. Phys. Soc.* **82** 633
Panissod P, Durand J and Budnick J I 1982 *Nucl. Instrum. Methods* **199** 99
Panissod P 1985 *Hyperfine Interact.* **124–126** 607
[32] Erich U 1969 *Z. Phys.* **227** 25
Ebert H, Winter H, Gyorffy B L, Johnson D D and Pinski F J 1988 *J. Phys. F: Met. Phys.* **18** 719
[33] Stadnik Z M, Griesbach P, Dehe G, Gütlich P and Maniawski F 1987 *J. Magn. Magn. Mater.* **70** 436
[34] Tansil J E, Obenshain F E and Czjzek G 1972 *Phys. Rev.* B **6** 2796
[35] Streever R L and Uriano G A 1966 *Phys. Rev.* **149** 295
[36] Stadnik Z M, Griesbach P, Dehe G, Gütlich P, Stroink G and Miyazaki T 1987 *Phys. Rev.* B **35** 8740
[37] Stadnik Z M, Wang P, Jansen N, Walcher D, Gütlich P and Kanomata T 2008 unpublished results